www.czasopisma.pan.pl PAN www.journals.pan.pl
Chemical and Process Engineering 2018, 39 (1), 39–57
DOI: 10.24425/119098

OPTIMAL FEED TEMPERATURE FOR AN IMMOBILIZED ENZYME FIXED-BED REACTOR: A CASE STUDY ON HYDROGEN PEROXIDE DECOMPOSITION BY COMMERCIAL CATALASE

Ireneusz Grubecki*

Faculty of Chemical Technology and Engineering, UTP University of Science and Technology,
3 Seminaryjna Street, 85-326 Bydgoszcz, Poland

Optimal feed temperature was determined for a non-isothermal fixed-bed reactor performing hydrogen peroxide decomposition by immobilized Terminox Ultra catalase. This feed temperature was obtained by maximizing the average substrate conversion under constant feed flow rate and temperature constraints. In calculations, convection-diffusion-reaction immobilized enzyme fixed-bed reactor described by a set of partial differential equations was taken into account. It was based on kinetic, hydrodynamic and mass transfer parameters previously obtained in the process of H_2O_2 decomposition. The simulation showed the optimal feed temperature to be strongly dependent on hydrogen peroxide concentration, feed flow rate and diffusional resistances expressed by biocatalyst effectiveness factor.

Keywords: optimal feed temperature, maximum hydrogen peroxide conversion, parallel deactivation, immobilized commercial catalase, diffusional resistances, fixed-bed reactor

1. INTRODUCTION

Fixed-bed reactors (FXBR) are important workhorses in biochemical industry because of their efficiency, low cost, and type of construction, operation, and maintenance. These (bio)reactors are widely employed since use of immobilized enzymes offers an easy product separation (with less allergenic enzyme impurities), less enzyme loss, increase in thermal and operational enzyme stability, enzyme protection against harmful environmental stress, and a better process control (Maria, 2012).

In general, the use of FXBR presents intrinsic kinetic advantages over stirred-tank reactors for most bioprocess types, ensuring higher rates and a lower risk to disintegrate the support through mechanical shearing.

Design and optimization of fixed-bed reactors are not an easy task and often involve an inherent trade-off between different and conflicting objectives (Sendín et al., 2006). These objectives, including economic benefits, investment, operating and materials costs, quality and control aspects, can be currently used to derive feasible optimal solutions for such a reactor, applying specific numerical algorithms, for example Pareto-optimal fronts method for pairs of adverse objectives (Maria and Crisan, 2017). Particularly, in case of bioprocesses, optimal conditions assurance can be a very challenging task (even if the process model is available) because of enzyme deactivation (which usually leads to decrease of reaction rate) which is not always taken into account to predict proper bioreactor behaviour (Al-Muftah and Abu-Reesh,

* Corresponding author, e-mail: ireneusz.grubecki@utp.edu.pl

2005; Hassan et al., 1995; Berendsen et al., 2007). The factors responsible for enzyme deactivation characteristics in relationship to the main enzyme catalysed reaction can be decisive in choosing the reactor operating mode (Maria and Crisan, 2015) and optimal operating conditions for biotransformations course (Grubecki, 2016). This optimal operating policy can be practically achieved mainly in two control modes of reactor operation. The first one is the control of feed rate to the (bio)reactor in such a way that it decreases with time in order to compensate the loss of enzyme activity (Maria and Crisan, 2015). The second mode is temperature as the most relevant variable to be optimized for enzyme reactor operation. At moderate temperatures the enzyme deactivation rate is insignificant while its initial reaction rate increases with temperature. At higher temperatures the concentration of active enzyme decreases due to the increase in the deactivation rate which becomes predominant. As a result, the reaction rate diminishes. Thus, the proper temperature strategy (e.g. optimal temperature control) should find a compromise between the rate of reaction and that of enzyme deactivation (Grubecki, 2012).

Most frequently optimal considerations deal with the processes occurring in the presence of (bio)catalyst that undergoes thermal deactivation (Polakovic and Vrabel, 1996).

Biocatalyst deactivation dependent on substrate concentration (parallel deactivation) is the specific one and makes enzyme activity both the function of time and position. Such deactivation mechanism is related to catalase which has intensively been applied for elimination of residual hydrogen peroxide in various domains such as textile (Soares et al., 2011), food (Farkye, 2004), and semiconductors industries (Oh et al., 2002), as well as wastewater treatment (Charron et al., 2004) and cosmetics and pharmaceutical formulations in biosensor system (Campanella et al., 1998; Görenek et al., 2004; O'Brien et al., 2007).

Catalase can be applied in the native form or immobilized on natural and synthetic carrier materials based on polymers or low molecular compounds, organic or inorganic ones (Grigoras, 2017). However, when working with immobilized enzymes (especially catalase), internal and/or external diffusional resistances (IDR/EDR) are likely to occur regardless of the method of immobilization used (Illanes A., 2013).

Hydrogen peroxide decomposition (HPD) by catalase has theoretically been studied (Do, 1984; Do and Weiland, 1981a; 1981b; 1981c; Hossain and Do, 1989; Grubecki, 2012) and verified experimentally (Alptekin et al., 2009; Cantemir et al., 2013; Costa et al., 2002; Krishna and Kittrell, 1990; Tai and Greenfield, 1981; Tarhan and Uslan, 1990; Trusek-Hołownia and Noworyta, 2015). However, in none of the papers the optimal operating policy ensuring the maximum of the time-averaged substrate conversion achieved in the fixed-bed reactor has been taken into account.

One can notice that the optimal temperature and/or flow rate control policies in a continuous packed-bed reactor are not easy to implement in industrial practice, because of the difficulties of controlling the substrate solution temperature as a function of time and reactor length.

The optimization problem of the fixed-bed reactor has been solved by Lin (1991) in relation to non-isothermal biotransformation occurring in the presence of immobilized enzyme undergoing thermal deactivation described by a first-order kinetic equation.

However, the analysis mentioned above is of a general nature, it does not take into account mass-transfer limitations. Moreover, hydrogen peroxide decomposition in industrial practice usually is carried out under isothermal conditions at temperatures above 323 K, though the optimal activity of catalase is achieved in the range of moderate temperatures (293–323K) (BRENDA data-base, 2018; Ene and Maria, 2012; Horst et al., 2006; Maria et al., 2012;). Thus, the key problem is to determine the temperature conditions in which the decomposition process of hydrogen peroxide should be performed taking into account lower and upper temperature constraints.

Hence, the objective of the present study was to search for – under constant feed flow rate – the optimal feed temperature (OFT) of the fixed-bed reactor performing hydrogen peroxide decomposition by Termi-

nox Ultra catalase (TUC), immobilized onto non-porous glass beads. The optimal feed temperature was obtained by maximizing time-averaged hydrogen peroxide conversion accounting for the lower $T_{\min}$ and the upper $T_{\max}$ temperature constraints as well as diffusional resistances expressed by global effectiveness factor.

The use of model solutions in the light of the conducted analysis can improve the knowledge of hydrogen peroxide decomposed by catalases from various sources (especially Terminox Ultra catalase) and the selection of operating conditions.

2. FORMULATION OF THE FIXED-BED REACTOR PROBLEM

Let us consider a packed-bed immobilized enzyme reactor of length, H, inner diameter, D_R, through which the hydrogen peroxide solution with feed flow rate Q, flows.

2.1. Assumptions

The course of any enzymatic process depends on a number of factors. These factors are usually difficult to measure, especially in the case of enzymatic systems. Thus, to formulate and then solve the mathematical model of FXBR in which the hydrogen peroxide decomposition by immobilized TUC is carried out, the following assumptions have been made:

- catalyst particles are spherical and uniformly packed inside the reactor;
- volume and density of the reacting medium are constant;
- the process is diffusion-controlled;
- effective diffusivity does not change throughout the particles and is independent of the substrate concentration;
- enzyme activity is uniform throughout the particle and the reactor;
- feed and pellet temperatures are constant;
- pressure drop across the reactor as well as radial concentration and temperature gradients in the bulk liquid are assumed to be negligible;
- substrate (hydrogen peroxide) transport rate from the bulk liquid to the outer surface of the immobilized bead is equimolar diffusion described by Equation (1) below

$$r_{\mathrm{m}} = k_{\mathrm{mL}}\, a_{\mathrm{m}} (C_{\mathrm{A}} - C_{\mathrm{As}}) \tag{1}$$

  where k_{mL} is the external mass transfer coefficient, a_{m} is the area of the external mass transfer, C_{A} and C_{As} are the H_2O_2 concentrations in the bulk and at the external surface of immobilized beads, respectively;
- rate of hydrogen peroxide decomposition, r_{A}, is described by the Michaelis–Menten kinetics

$$r_{\mathrm{A}} = \eta_{\mathrm{eff}} k'_{\mathrm{R}} \frac{C_{\mathrm{E}} C_{\mathrm{A}}}{(1 + C_{\mathrm{A}}/K_{\mathrm{M}})} \tag{2}$$

- effect of hydrogen peroxide concentration on the enzyme deactivation rate, r_{D}, in agreement with Do and Weiland theory (1980) and verified by Vasudevan and Weiland (1990) has been taken into account

$$r_{\mathrm{D}} = \eta_{\mathrm{eff}} k_{\mathrm{D}} \frac{C_{\mathrm{E}} C_{\mathrm{A}}}{(1 + C_{\mathrm{A}}/K_{\mathrm{D}})} \tag{3}$$

- in industrial practice hydrogen peroxide decomposition is carried out at low H_2O_2 concentration (lower or equal to 0.02 kmol m^{-3}),
- effect of temperature on the rate constants for reaction $\nu_R(k_R)$ and deactivation $\nu_D(k_D)$ is expressed by the Arrhenius equation

$$k_i = k_{i0} \exp\left(-\frac{E_i}{RT}\right) \qquad (i = \mathrm{D},\ \mathrm{R}) \tag{4}$$

2.2. Fixed-bed reactor model

2.2.1. Mass and energy balances with enzyme deactivation rate equation

To make the numerical simulation easy the following dimensionless state variables

$$\overline{C}_E = \frac{C_E}{C_{E0}}, \qquad \overline{C}_A = \frac{C_A}{C_{A,In}}, \qquad \vartheta = \frac{T}{T_{In}} \tag{5}$$

dimensionless axial coordinate variable and dimensionless utilization time of biocatalyst

$$z = \frac{h}{H}, \qquad \tau = t\frac{U_S}{H} \tag{6}$$

as well as dimensionless process parameters

$$\mathrm{Pe}_{mL} = \frac{U_S H}{\varepsilon D_L}, \qquad \mathrm{Pe}_{qL} = \frac{\rho C_P U_S H}{\varepsilon \Lambda_{ax}} \tag{7a}$$

$$\mathrm{K}_1 = k_R a_m \frac{H}{U_S}, \qquad \mathrm{K}_2 = k_D C_{A,In} \frac{H}{U_S} \tag{7b}$$

$$\mathrm{H}_R = \frac{(-\Delta H_R) C_{A,In}}{\rho C_P T_{In}}, \qquad \beta_i = \frac{E_i}{RT_{In}} \quad (i = \mathrm{D},\ \mathrm{R}) \tag{7c}$$

were introduced.

Then, under the above assumptions, the differential mass and energy balances in the bulk liquid phase for substrate as well as equation describing the enzyme (TUC) deactivation rate can be written as:

$$\varepsilon \frac{\partial \overline{C}_A}{\partial \tau} = \mathrm{Pe}_{mL}^{-1} \frac{\partial^2 \overline{C}_A}{\partial z^2} - \frac{\partial \overline{C}_A}{\partial z} - \eta_{eff}(1-\varepsilon)\mathrm{K}_1 \overline{C}_E \overline{C}_A \tag{8}$$

$$\varepsilon \frac{\partial \vartheta}{\partial \tau} = \mathrm{Pe}_{qL}^{-1} \frac{\partial^2 \vartheta}{\partial z^2} - \frac{\partial \vartheta}{\partial z} - \eta_{eff}(1-\varepsilon)\mathrm{K}_1 \mathrm{H}_R \overline{C}_E \overline{C}_A \tag{9}$$

$$-\frac{\partial \overline{C}_E}{\partial \tau} = \eta_{eff}(1-\varepsilon)\mathrm{K}_2 \overline{C}_E \overline{C}_A \tag{10}$$

The initial ($\tau = 0$) and boundary conditions for Eqs. (8)–(10) at the entry ($z = 0$) and exit ($z = 1$) of the bioreactor are given by:

$$\tau = 0, \quad 0 \le z \le 1: \qquad \overline{C}_A = \overline{C}_E = \vartheta = 1 \tag{11}$$

$$\tau > 0, \quad z = 0: \qquad \mathrm{Pe}_{mL}^{-1} \frac{\partial \overline{C}_A}{\partial z} = \overline{C}_A - 1, \quad \mathrm{Pe}_{qL}^{-1} \frac{\partial \vartheta}{\partial z} = \vartheta - 1 \tag{12}$$

$$\tau > 0, \quad z = 1: \qquad \frac{\partial \overline{C}_A}{\partial z} = \frac{\partial \vartheta}{\partial z} = 0 \tag{13}$$

2.2.2. Calculation of the effectiveness factor

To evaluate the effectiveness factor (η_{eff}) appearing in Eqs. (2), (3) and (8)–(10), the following expressions can be adopted (Illanes et al., 2013)

$$\eta_{\text{EDR}} = (1+\text{Da})^{-1} \qquad \text{effect of EDR} \tag{14a}$$

$$\eta_{\text{IDR}} = \phi^{-1}\left[\tanh^{-1}(3\phi) - (3\phi)^{-1}\right] \qquad \text{effect of IDR} \tag{14b}$$

$$\eta_{\text{G}} = \frac{\text{Bi}\left[\tanh^{-1}(3\phi) - (3\phi)^{-1}\right]}{\phi\left[\text{Bi} - 1 + 3\phi\tanh^{-1}(3\phi)\right]} \qquad \text{effect of EDR and IDR} \tag{14c}$$

In order to calculate the Damkőhler (Da) and Biot (Bi) numbers the external mass transfer model developed by the author in a the previous work (Grubecki, 2017) has been applied. When $\text{Bi} \to \infty$, then a system is free of EDR and Eq. (14c) takes the form of Eq. (14b).

It is obvious that when enzyme deactivation occurs the effectiveness factor tends to increase, because the lower biocatalyst activity moves the system away from mass-transfer limitations (Palazzi and Converti, 2001). Thus, the evaluation of the diffusional resistances in a reactor utilizing a biocatalyst subject to deactivation (especially parallel deactivation) can be a very hard problem, even from a numerical solution viewpoint. Thus, in this work calculations have been made for the lowest value of effectiveness factor η_{eff} corresponding to the initial biocatalyst activity (Eqs. (14a)–(14c)).

To assess the effectiveness factor (η_{eff}) in the present work, the relationships suggested by Doran (1995) and used by Maria and Crisan (2015) can be applied as well. However, it should be noticed, that for biotransformations occurring at low substrate concentrations ($K_{\text{M}}/C_{\text{A,In}} \to \infty$), the Michaelis-Menten kinetics can be expressed by a first-order kinetic equation and the relationships described by Doran (1995) take the form of Eqs. (14a)–(14c).

2.2.3. Estimation of film mass transfer coefficient

To predict the mass-transfer coefficient for H_2O_2 the following correlation developed by Chilton and Colburn (1934) was used

$$k_{\text{mL}} = K\frac{D_{\text{L,S}}^{2/3}}{d_{\text{P}}^{1-n}}\left(\frac{\rho}{\eta}\right)^{(n-1/3)} U_{\text{S}}^{n} \tag{15}$$

This correlation was verified experimentally for hydrogen peroxide decomposed by Terminox Ultra catalase in a model fixed-bed reactor (Grubecki, 2017). Consequently, the values of n and K were assessed to be equal to 0.632 and 0.972, respectively. Equation (15) is applicable for $0 < \text{Re} < 20$.

2.2.4. Calculation of effective diffusion coefficient

To show the role of porosity on diffusion, free diffusivity in a fluid without obstacles must be scaled with tortuosity, i.e. the diffusion path of species accounting for the deviation from straight line. In this paper, the frequently used tortuosity-porosity relation (Karger and Ruthven, 1992; Sherwood et al., 1975) was applied to estimate the effective diffusivity

$$D_{\text{eff}} = D_{\text{L,S}}\frac{\varepsilon_{\text{P}}}{\tau_{\text{P}}} \tag{16}$$

where τ_P is tortuosity factor expressed as follows (Shen and Chen, 2007):

$$\tau_P^2 = \frac{\varepsilon_P}{1-(1-\varepsilon_P)^{1/3}} \tag{17}$$

and ε_P is the effective, transport-through porosity of the considered structure assumed to be 0.5 (Do and Hossain, 1987).

2.2.5. Correlations for the dispersion coefficients

The Péclet number for mass transfer (Pe_{mL}) as a function of Reynolds number (Re) was developed from tracer experiments to be (Appendix A)

$$Pe_{mL} = 0.484Re + 1.420 \tag{18}$$

The experimental correlation (Eq. (19)) describing the effect of Reynolds and Prandtl numbers on the thermal dispersion coefficient (Λ_x) and developed by Testu et al. (2007) was used in calculations to determine the Péclet number for heat transfer Pe_{qL}

$$\Lambda_x = 1.3 + 0.607\varepsilon(1-\varepsilon)Re^{1.5}\left[\frac{8.87(Pr-0.7)-0.543(Pr-7.02)}{6.32}\right] \tag{19}$$

This correlation should be applied for water/glass beads and air/glass bead systems in the $0 < Re \leq 130$ range.

2.3. Objective function

An optimizing problem has been formulated that under constant feed flow rate would provide a feed temperature maximizing the following time-averaged substrate conversion

$$\alpha_{m,z=1} = \frac{1}{\tau_f}\int_0^{\tau_f}\left[1-\overline{C}_A(z=1,x)\right]dx \tag{20}$$

2.4. Constraints

To ensure a safe operation the bioreactor temperature and feed flow rate, Q, are bounded as below

$$\vartheta_{min} \leq \vartheta \leq \vartheta_{max} \tag{21}$$

$$Q_{min} \leq Q \leq Q_{max} \tag{22}$$

3. RESULTS AND DISCUSSION

The optimal feed temperature maximizing the time-averaged hydrogen peroxide conversion was obtained using constrained non-linear minimization with MATLAB Optimization Toolbox (Mathworks Inc., Natick

MA, USA). In optimization procedure, the MATLAB Partial Differential Equation Toolbox was employed to solve a set of non-linear partial differential equations (Eqs. (8)–(10)).

To perform the calculations, the rate constants for reaction and deactivation were earlier determined (Grubecki, 2017) from data collected during a laboratory study carried out at different temperatures in model FXBR (Table 1) for the process of HPD by immobilized TUC onto non-porous glass beads. These rate constants have been illustrated in Fig. 1.

Table 1. Characteristics of the model reactor and biocatalyst employed in calculations

Reactor sizes	
Length (m)	0.36
Diameter ($\times 10^{-3}$ m)	8.00
Cross section ($\times 10^{-5}$ m^2)	5.03
Total volume ($\times 10^{-5}$ m^3)	1.81
External surface/reactor volume unity ($\times 10^{3}$ m^{-1})	8.32
Bed characteristics	
Particle diameter ($\times 10^{-4}$ m)	5.05
Bed density ($\times 10^{3}$ kg m^{-3})	1.82
Total biocatalyst weight in reactor ($\times 10^{-3}$ kg)	33.0
Total biocatalyst volume in reactor ($\times 10^{-6}$ m^3)	12.67
Free volume ($\times 10^{-3}$ m^3)	5.43
Porosity	0.30

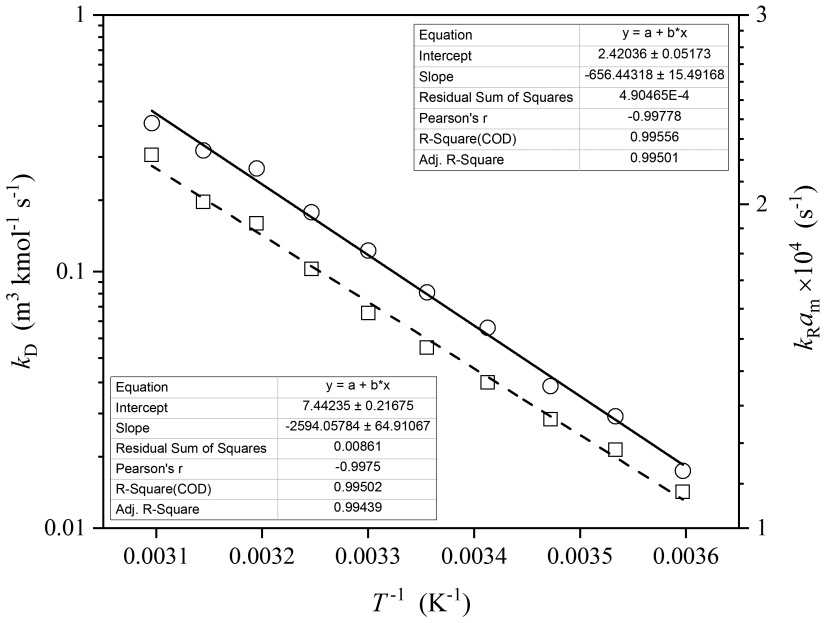

Fig. 1. Dependences of $k_R a_m$ (solid line) and k_D (dashed line) vs. (T^{-1}) for HPD by TUC

Then, the activation energies and frequency factors for reaction and deactivation were calculated and listed in Table 2.

Table 2. Kinetic parameters in Arrhenius equation for reaction and deactivation

Reaction of hydrogen peroxide decomposition	
Activation energy (kJ mol^{-1})	$E_R = 12.6 \pm 0.3$
Frequency factor (s^{-1})	$k_{R0} a_m = 48.00 \pm 5.38$
Deactivation of Terminox Ultra catalase	
Activation energy (kJ mol^{-1})	$E_D = 49.7 \pm 1.2$
Frequency factor (m^3 kmol^{-1} s^{-1})	$k_{D0} = (2.77 \pm 1.08) \times 10^7$

Furthermore, in calculations, the reaction heat $(-\Delta H_R)$ of HPD of 93 kJ mol^{-1} (Eissen et al., 2003; Berendsen et al., 2007) has been employed.

It is apparent from Eqs. (8)–(10) that the biotransformation occurring in the presence of immobilized enzyme is governed by the parameters, $C_{A,In}$, T_{In}, K_1, K_2, H_R and η_{eff} considered to be of crucial importance.

When working with immobilized enzymes, analysis assessing mass-transfer limitations should be conducted. They are usually expressed as external or/and internal diffusional resistances (EDR/IDR). Thus, the values of the Biot number, Bi, and Thiele modulus, ϕ, are listed in Table 3, while the corresponding behavior of the effectiveness factors $\eta_{EDR} = \eta_{EDR}(Q,T)$ and $\eta_G = \eta_G(Q,T)$ obtained by Eqs. (14a) and (14c), respectively, are shown in Figs. 2a and 2b.

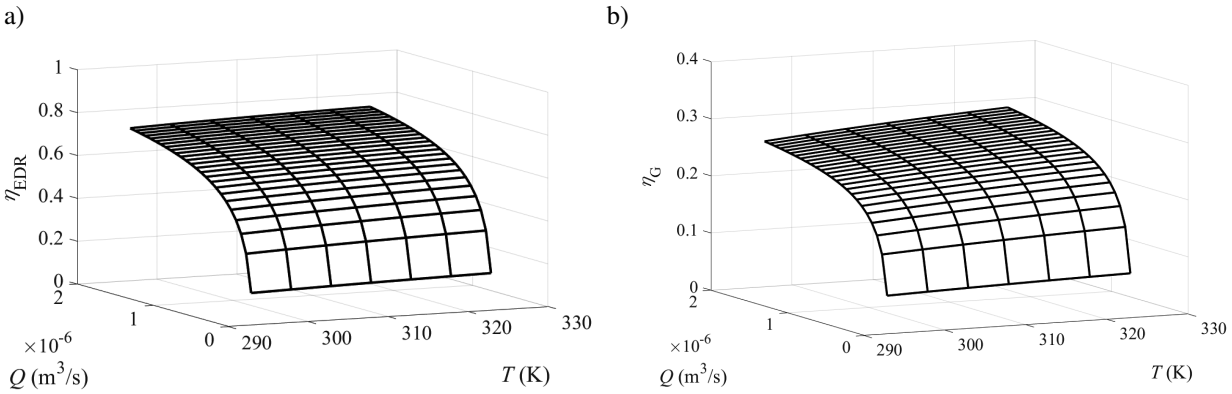

Fig. 2. Effectiveness factor η_{eff} under a) external diffusional restrictions $\eta_{eff} = \eta_{EDR}$, b) external and internal diffusional resistances $\eta_{eff} = \eta_G$, as a function of volumetric flux (Q) and temperature (T)

Assessing the Biot number (Table 3), for $Q \geq 25 \times 10^{-8}$ m^{3}s^{-1} the EDR can be disregarded and rate of HPD can be controlled by IDR slightly decreasing with temperature ($\eta_{IDR} = 0.33$ for $T_{min} = 293$ K and $\eta_{IDR} = 0.37$ for $T_{max} = 323$ K). On the contrary, when $Q \leq 25 \times 10^{-8}$ m^{3}s^{-1} the combined effect of EDR and IDR takes place. Thus, to express the impact of diffusional resistances in the whole range of Q, the global effectiveness factor should be introduced (Fig. 2b). Variations of Q ranging from 166.7×10^{-8} to 1.67×10^{-8} m^{3}s^{-1} cause the decrease of the global effectiveness factor, η_G, from 0.30 to 0.072.

Thiele modulus has been calculated for intrinsic reaction rate constant of HPD (Table 2). Thus, it takes its maximum value shown in Table 3, and in consequence, the effectiveness factor under IDR, η_{IDR}, takes

Table 3. The value of Biot number, Bi, and Thiele modulus, ϕ, estimated at different values of volumetric flux, Q, as well as lower T_{min} and upper T_{max} temperature constraints

$Q \times 10^8$ m^{3}s^{-1}	$T_{min} = 293$ K		$T_{max} = 323$ K	
	Bi	ϕ	Bi	ϕ
166.7	31.1	2.590	29.4	2.314
125.0	25.9		24.5	
83.3	20.1		19.0	
41.7	13.0		12.2	
25.0	9.38		8.86	
16.7	7.26		6.86	
8.33	4.68		4.43	
3.33	2.62		2.48	
1.67	1.69		1.60	

the minimum value. Therefore, the global effectiveness factor applied in this work may be useful in the process of HPD by catalase originating from various sources.

To determine the optimal temperature strategies, especially OFT, which enable the maximum performance of the reactor, the temperature distribution in the bulk reaction medium can be particularly useful. In such analysis, the energy balance and the allowable temperature range should be taken into consideration. For Terminox Ultra catalase such temperature range is from $T_{min} = 293$ K to $T_{max} = 323$ K due to its optimal operational activity (Grubecki, 2016).

Analysis revealed that the reaction heat of HPD by TUC released at low H_2O_2 concentrations makes the temperature rise along the length of bioreactor negligible so temperature conditions in the reactor can be considered as isothermal.

On the other hand, the temperature distribution in the bed is independent of the reaction heat. Thus, it allows to predict temperature conditions existing in bulk liquid phase. What does change is the value of the maximum temperature reached in the reactor and at higher H_2O_2 concentration, it may be higher by a few to even dozen or so degrees in comparison with the feed temperature, T_{In}. The higher the feed H_2O_2 concentration, the faster deactivation of TUC can be expected. As a result, the most significant temperature growth is achieved only during the initial run of the bioreactor.

It can be noted that for analysed values of kinetic and mass-transfer parameters such feed temperature (e.g. optimal feed temperature, $T_{In,opt}$) can be indicated, for which average H_2O_2 conversion at reactor outlet attains maximum value (Fig. 3, lines 2–8) or is the highest one (Fig. 3, line 1).

Generally, the lower the feed H_2O_2 concentration (Fig. 4), the value of global effectiveness factor as well as the higher enzyme activity (Fig. 5), the higher the temperature $(T_{In,opt})$, that yields the maximum (or highest) level of average H_2O_2 conversion at the reactor outlet (Eq. (20)). It should be noted however, that the optimal feed temperature, $T_{In,opt}$, exists only for a certain number (at least one) of effectiveness factor, $\eta_G = \eta_G^*$. Then, the average H_2O_2 conversion curve has only one, very weak peak. In case under consideration the above mentioned factors are equal: $\eta_G^* = 0.168$ for $Q^* = 11.7 \times 10^{-8}$ m^3 s^{-1}, $\eta_G^* = 0.159$ for $Q^* = 10 \times 10^{-8}$ m^{3}s^{-1}, $\eta_G^* = 0.149$ for $Q^* = 8.33 \times 10^{-8}$ m^{3}s^{-1} and $\eta_G^* = 0.137$ for $Q^* =$

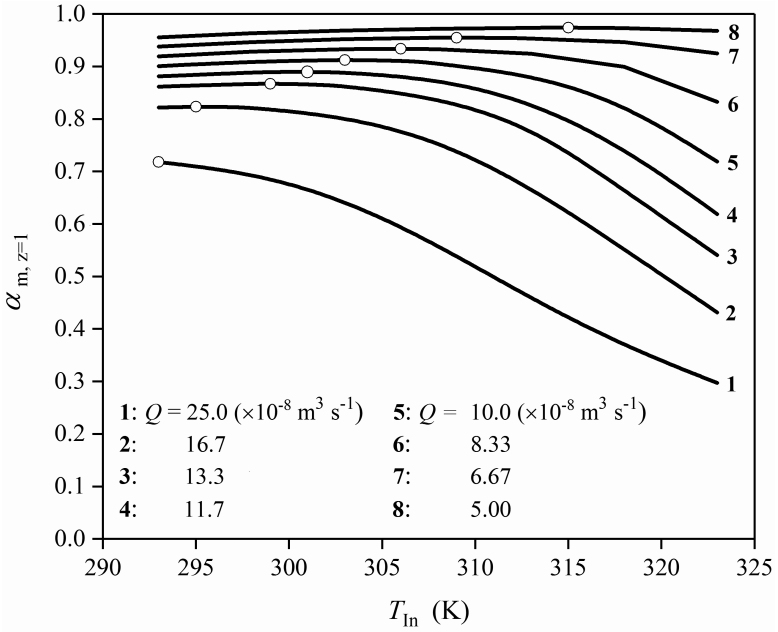

Fig. 3. Exemplary figure showing the effect of feed temperature T_{In} and volumetric flux, Q, on average conversion of hydrogen peroxide decomposed by TUC in the adiabatic reactor. Open circles represent the maximum (or the highest) value

6.67×10^{-8} m^{3}s^{-1}. For $\eta_G > \eta_G^*$ (in this case $\eta_G > 0.168$), an average substrate conversion decreases with raising temperature, T_{In}, and then the OFT is equal to lower temperature constraint $T_{In,opt} = T_{min}$. On the contrary, for $\eta_G < \eta_G^*$ (in this case $\eta_G < 0.137$), an average H_2O_2 conversion increases with raising temperature, T_{In}, and the OFT should be equal to upper temperature constraint ($T_{In,opt} = T_{max}$). It means that under such circumstances the reactor should operate under isothermal conditions at the temperature level of T_{max}. The heat effect of reaction does not affect the value of $T_{In,opt}$.

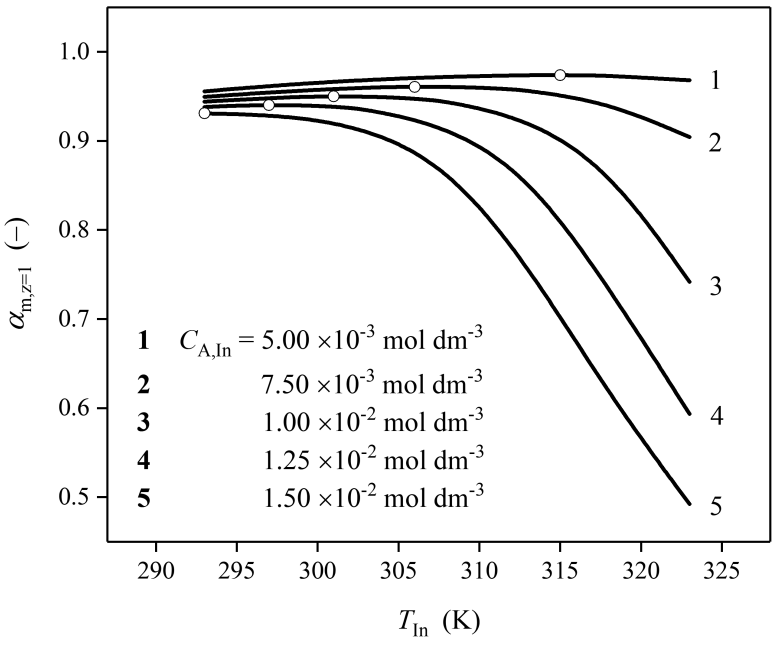

Fig. 4. Effect of feed temperature (T_{In}) and feed concentration ($C_{A,In}$) on the average H_2O_2 conversion at the reactor outlet (open circles represent the maximum value)

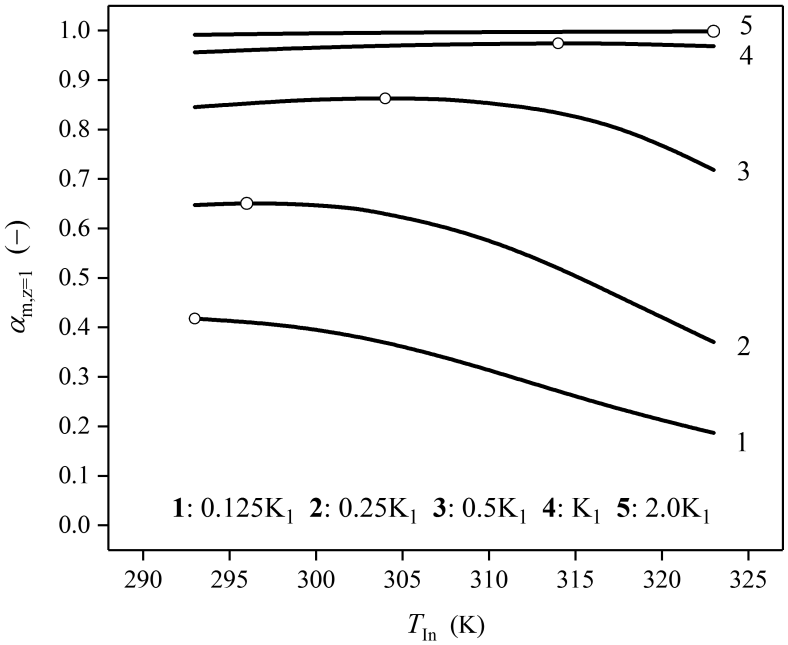

Fig. 5. Effect of feed temperature (T_{In}) and enzyme activity (K_1) on the average H_2O_2 conversion at the reactor outlet (open circles represent the maximum value)

A biocatalyst of a larger size provides greater diffusional resistances and a decrease of the global effectiveness factor. As a result, an increase of OFT value can be expected. For clarity purposes, the dependence $\alpha_{m,z=1}$ vs. T_{In} and d_P has been shown in Fig. 6. For example, increase of the biocatalyst pellet diameter from 5×10^{-4} to 10×10^{-4} m causes the OFT rise from 314 K to 318 K, respectively, for $Q = 5 \times 10^{-8}$ m^{3}s^{-1}, and from 303 K to 307 K, respectively, for $Q = 10 \times 10^{-8}$ m^{3}s^{-1}.

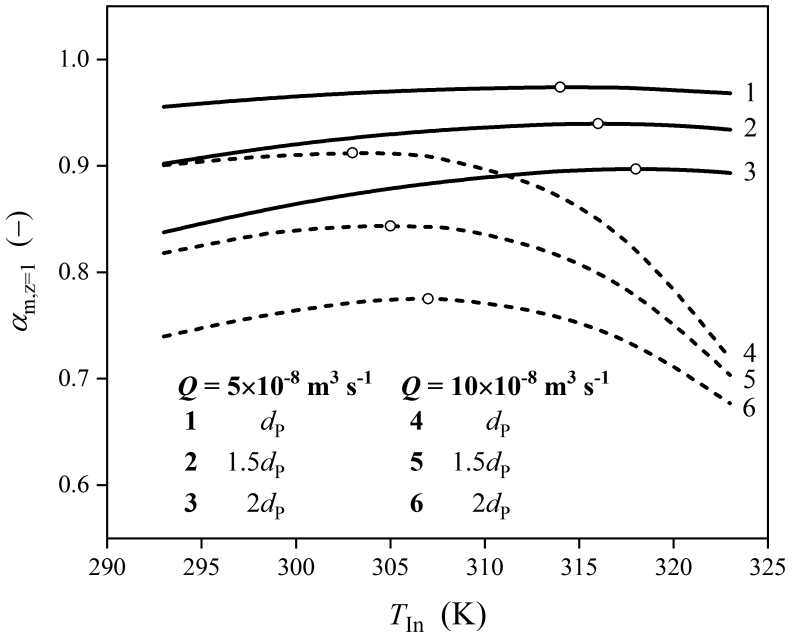

Fig. 6. Effect of feed temperature (T_{In}) and particle diameter (d_P) on the average H_2O_2 conversion at the reactor outlet (open circles represent the maximum value). Solid lines represent conversion for $Q = 5 \times 10^{-8}$ m^{3}s^{-1} and dashed line for $Q = 10 \times 10^{-8}$ m^{3}s^{-1}

When the effect of external film diffusion can be disregarded then the process course is controlled by IDR related to the internal structure of biocatalyst. Figure 7 depicts the dependence illustrating the effect of effectiveness factor under IDR, η_{IDR}, and volumetric flux, Q, on OFT. Due to clarity of Fig. 7, the relationship $T_{In,opt}$ vs. η_{IDR} has been presented only for selected values of $Q \times 10^8$ equals 3.33, 8.33, 16.7, 25.0 m^3s^{-1}, for which the differences in curve courses are substantial.

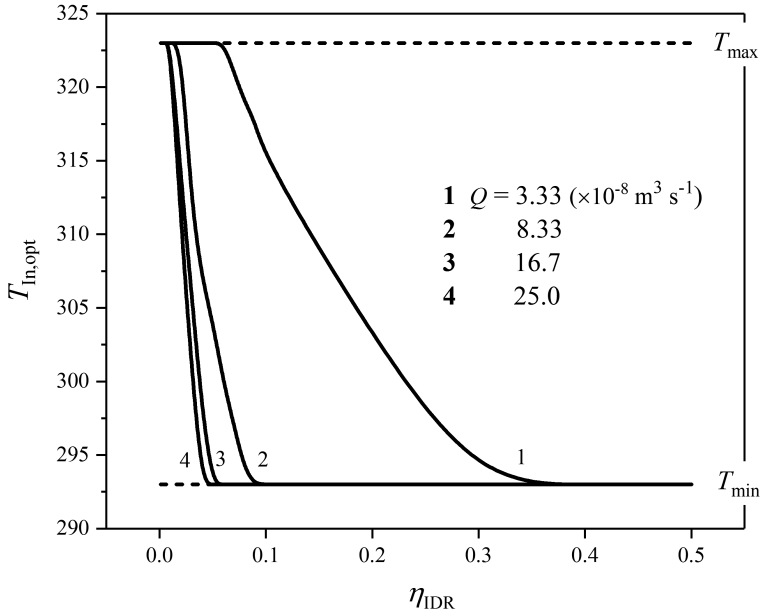

Fig. 7. Exemplary figure showing effect of effectiveness factor under IDR (η_{IDR}) and volumetric flux (Q) on OFT ensuring the maximum average substrate conversion ($\alpha_{m,z=1}$) at the reactor outlet

Generally, in a situation when EDR can be negligible (similarly when the combined effect of EDR and IDR occurs), for any volumetric flux Q, such values of $\eta_{IDR} = \eta^*_{IDR}$ can be indicated that for $\eta_{IDR} > \eta^*_{IDR}$, the optimal feed temperature $T_{In,opt}$ is equal to T_{min}. However, for $\eta_{IDR} < \eta^*_{IDR}$, $T_{In,opt} = T_{max}$. Flow slowdown causes shift of the η^*_{IDR} values toward the higher ones.

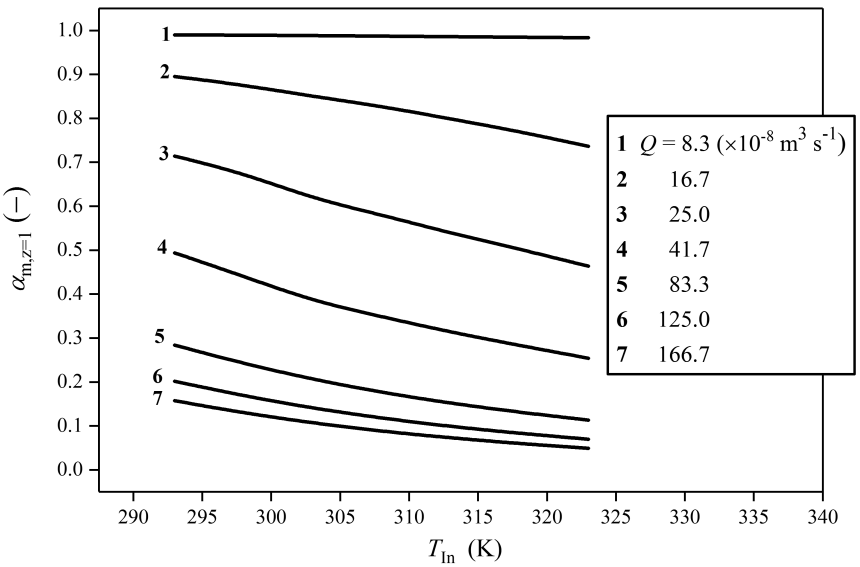

Fig. 8. Exemplary figure showing effect of feed temperature (T_{In}) and volumetric flux (Q) on average H_2O_2 conversion ($\alpha_{m,z=1}$) for $\eta_{IDR} = 0.354$

Especially, for HPD the value of effectiveness factor $\eta_{IDR} = 0.354$ under IDR has been assumed. It was estimated from Eq. (14b) for kinetic and mass-transfer parameters considered in this work and calculated for moderate temperature of 303 K. Figure 8 demonstrates the effect of feed temperature, T_{In}, and volumetric flux, Q, on average H_2O_2 conversion, $\alpha_{m,z=1}$, at the reactor outlet for the assumed value of effectiveness factor (η_{IDR}).

It may be noticed that when in process of HPD the biocatalyst is applied for which $\eta_{IDR} = 0.354$, the OFT maximizing the average H_2O_2 conversion at reactor outlet, is the lower allowable temperature $T_{min} = 293$ K. The use of biocatalyst of η_{IDR} value lower than 0.354 increases temperature $T_{In,opt}$ (Fig. 7).

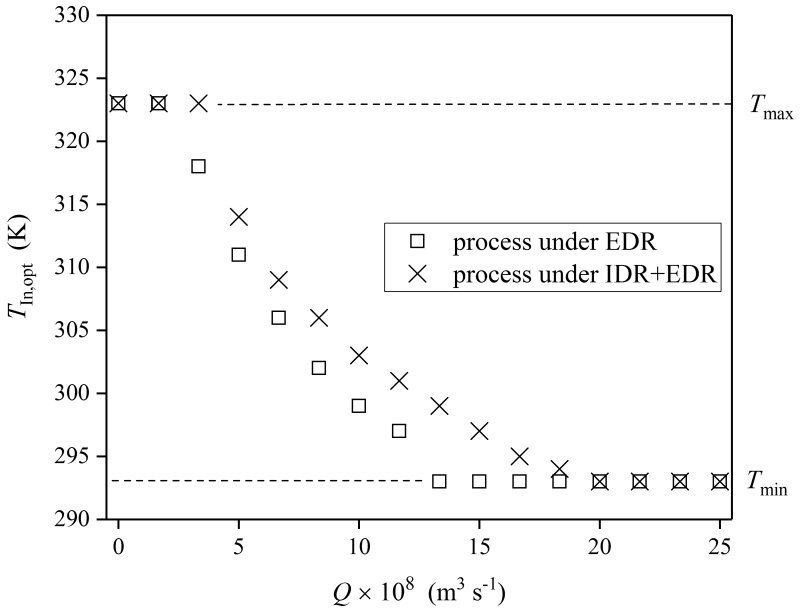

Fig. 9. Optimal feed temperature $(T_{In,opt})$ vs. feed flow rate (Q) for the process under EDR as well as combined EDR and IDR effect. Variations of $Q \times 10^8$ ranging from 25.0 m^3s^{-1} to 1.67 m^3s^{-1} cause the decrease of η_{EDR} and η_G from 0.512 to 0.160 and from 0.21 to 0.074, respectively

If the enzyme is immobilized on a carrier surface, then – for the same feed flow rate Q – the effectiveness factor under EDR (Eq. (14a)), takes always a higher value when compared with the global one (η_G) considered earlier (Figs. 2a and 2b). Consequently, OFT for the process under EDR takes the lower values than those required for the process under the combined effect of IDR and EDR (Fig. 9).

4. CONCLUSIONS

Based on the presented simulation study carried out for parametric values the following conclusions can be drawn:

- The external diffusional resistances in the process of hydrogen peroxide decomposition by immobilized TUC should be always taken into account. In consequence, the global effectiveness factor should be used to express the combined effect of EDR and IDR. When the volumetric flux $(Q \times 10^8)$ varies from 166.7 m^3s^{-1} to 1.67 m^3s^{-1} (for the fixed value of $\eta_{IDR} = 0.354$) effectiveness factor under EDR and the global one take the values from $\eta_{EDR} = 0.777$ and $\eta_G = 0.288$ to $\eta_{EDR} = 0.227$ and $\eta_G = 0.074$, respectively.

- For each value of volumetric flux analyzed in this work, one can indicate a certain limit value of the effectiveness factor, η^*_{eff}, that for $\eta_{\mathrm{eff}} > \eta^*_{\mathrm{eff}}$ the average H_2O_2 conversion at the reactor outlet, $\alpha_{\mathrm{m,z=1}}$, increases when feed temperature T_{In} rises, while $\alpha_{\mathrm{m,z=1}}$ decreases for $\eta_{\mathrm{eff}} < \eta^*_{\mathrm{eff}}$. Thus, there exists such a feed temperature value $T_{\mathrm{In,opt}}$, for which the average H_2O_2 conversion is the maximal (for η^*_{eff}) or the highest (for other values η_{eff}). The higher diffusional resistances, the higher the temperature ensuring the average maximum H_2O_2 conversion.
- The higher enzyme activity and the lower feed concentration, the higher optimal feed temperature and hydrogen peroxide conversion can be achieved.
- The rise of the biocatalyst particle size causes the increase of the diffusional resistances, and optimal feed temperature as a consequence. Additionally, this temperature rise compensates reduction in H_2O_2 conversion caused by decrease in specific surface area of the biocatalyst. Slowdown of the feed flow rate contributes toward the optimal feed temperature increase and substrate conversion at the same time.
- Analysis developed in this work allows relatively easily to determine the operating conditions (feed temperature and flow rate) at which productivity of the fixed-bed reactor for hydrogen peroxide decomposition by immobilized catalase achieves the maximum value or the highest one.

SYMBOLS

a_{m}	external surface area for mass transfer, $\mathrm{m^2\ m^{-3}}$
Bi	Biot number $(= k_{\mathrm{mL}} d_{\mathrm{P}} / 6 D_{\mathrm{eff}})$
C_{A}	bulk substrate concentration, $\mathrm{kmol\ m^{-3}}$
$C_{\mathrm{A},j}$	H_2O_2 concentration at the inlet ($j = \mathrm{In}$) and outlet ($j = \mathrm{Out}$), $\mathrm{kmol\ m^{-3}}$
C_{E}	enzyme activity, $\mathrm{kg\ m^{-3}}$
C_{P}	heat capacity for the bulk liquid, $\mathrm{J\ kg^{-1}\ K^{-1}}$
d_{P}	particle diameter, m
$D_{\mathrm{L,S}}$	substrate diffusivity, $\mathrm{m^2\ s^{-1}}$
D_{eff}	effective diffusion coefficient, $\mathrm{m^2\ s^{-1}}$
Da	Damköhler number $(= k_{\mathrm{R}} / k_{\mathrm{mL}})$
E_i	activation energy for reaction ($i = \mathrm{R}$) and deactivation ($i = \mathrm{D}$), $\mathrm{J\ mol^{-1}}$
H	bed depth, m
h	distance from reactor inlet, m
$\mathrm{H_R}$	dimensionless heat of reaction $(= (-\Delta H_{\mathrm{R}}) C_{\mathrm{A,In}} / \rho C_{\mathrm{P}} T_{\mathrm{In}})$
$(-\Delta H_{\mathrm{R}})$	heat of reaction, $\mathrm{J\ mol^{-1}}$
$\mathrm{K_1}$	dimensionless number, $(= k_{\mathrm{R}} a_{\mathrm{m}} H / U_{\mathrm{S}})$
$\mathrm{K_2}$	dimensionless number, $(= k_{\mathrm{D}} C_{\mathrm{A,In}} H / U_{\mathrm{S}})$
K_i	Michaelis constant for reaction ($i = \mathrm{R}$) and deactivation ($i = \mathrm{D}$), $\mathrm{kmol\ m^{-3}}$
k_{mL}	mass transfer coefficient, $\mathrm{m\ s^{-1}}$
k_{D}	modified rate constant for deactivation $(= \nu_{\mathrm{D}} / K_{\mathrm{D}})$, $\mathrm{m^3 kmol^{-1}\ s^{-1}}$
k_{D0}	pre-exponential factor for deactivation rate constant, $\mathrm{m^3 kmol^{-1}\ s^{-1}}$
k'_{R}	modified rate constant for reaction $(= \nu_{\mathrm{R}} / K_{\mathrm{M}})$, $\mathrm{m^3\ kg^{-1}\ s^{-1}}$
k_{R0}	pre-exponential factor for enzymatic reaction rate constant, $\mathrm{m\ s^{-1}}$
k_{R}	modified rate constant for reaction $(= k'_{\mathrm{R}} C_{\mathrm{E0}} / a_{\mathrm{m}})$, $\mathrm{m\ s^{-1}}$
$\mathrm{Pe_{mL}}$	Péclet number for mass transfer $(= U_{\mathrm{S}} H / \varepsilon D_{\mathrm{L}})$

Pe_{qL}	Péclet number for heat transfer $(= \rho c_P U_S H/\varepsilon\Lambda_x)$
Pr	Prandtl number $(= C_P\eta/\lambda)$
Q	feed flow rate, m^3s^{-1}
r_m	mass transfer rate, kmol $m^{-3}s^{-1}$
r_A	reaction rate, kmol $m^{-3}s^{-1}$
t	biocatalyst age, s
T_{In}	feed temperature, K
U_S	superficial velocity, m s^{-1}
z	dimensionless distance from reactor inlet $(= h/H)$

Greek letters

β_i	dimensionless Arrhenius number defined as $(= E_i/RT_{In})$ $(i = D, R)$
ε	porosity of the porous medium (= 0.3)
ϕ	Thiele modulus
η	fluid viscosity, kg $m^{-1}s^{-1}$
η_{eff}	effectiveness factor defined by Eqs. (14a)–(14c)
Λ_x	axial heat conduction in liquid phase, W $m^{-1}K^{-1}$
λ	liquid thermal conductance, W $m^{-1}K^{-1}$
ν_D	rate constant for deactivation, s^{-1}
ν_R	rate constant for reaction, kmol $kg^{-1}s^{-1}$
ρ	liquid density, kg m^{-3}
τ	dimensionless time $(= tU_S/H)$
ϑ	dimensionless state variable $(= T/T_{In})$

REFERENCES

Al-Muftah A.E., Abu-Reesh I.M., 2005. Effects of internal mass transfer and product inhibition on a simulated immobilized enzyme-catalyzed reactor for lactose hydrolysis. *Biochem. Eng. J.*, 23, 139–153. DOI: 10.1016/j.bej.2004.10.010.

Alptekin Ö., Tükel S.S., Yıldırım D., Alagöz D., 2009. Characterization and properties of catalase immobilized onto controlled pore glass and its application in batch and plug-flow type reactors. *J. Mol. Catal. B: Enzym.*, 58, 124–131. DOI: 10.1016/j.molcatb.2008.12.004.

Berendsen W.R., Lapin A., Reuss M., 2007. Non-isothermal lipase-catalyzed kinetic resolution in a packed bed reactor: Modeling, simulation and miniplant studies. *Chem. Eng. Sci.*, 62, 2375–2385. DOI: 10.1016/j.ces.2007.01.006.

BRENDA data-base. Available at: http://www.brenda-enzymes.org/enzyme.php?ecno=1.11.1.6

Campanella L., Roversi R., Sammartino M.P., Tomassetti M., 1998. Hydrogen peroxide determination in pharmaceutical formulations and cosmetics using a new catalase biosensor. *J. Pharm. Biomed. Anal.*, 18, 105–116. DOI: 10.1016/S0731-7085(98)00155-1.

Cantemir A. R., Raducan A., Puiu M., Oancea D., 2013. Kinetics of thermal inactivation of catalase in the presence of additives. Process Biochem., 48, 471–477. DOI: 10.1016/j.procbio.2013.02.013.

Charron I., Féliers C., Couvert A., Laplanche A., Patria L., Requieme B., 2004. Use of hydrogen peroxide in scrubbing towers for odor removal in wastewater treatment plants. *Water Sci. Technol.*, 50(4), 267–274.

Chilton T.H., Colburn A.P., 1934. Mass transfer (absorption) coefficients predictions from data on heat transfer and fluid friction. *Ind. Eng. Chem.*, 26, 1183–1187. DOI: 10.1021/ie50299a012.

Costa S.A., Tzanov T., Filipa Carneiro A., Paar A., Gübitz G.M., Cavaco-Paulo A., 2002. Studies of stabilization of native catalase using additives. *Enzyme Microb. Technol.*, 30, 387–391. DOI: 10.1016/S0141-0229(01)00505-1.

Do D.D., Weiland R.H., 1981a. Self-poisoning in single catalyst pellets. *Ind. Eng. Chem. Fundam.*, 20, 34–41. DOI: 10.1021/i100001a007.

Do D.D., Weiland R.H., 1981b. Fixed bed reactors with catalyst poisoning: First order kinetics. *Chem. Eng. Sci.*, 36, 97–104. DOI: 10.1016/0009-2509(81)80051-6.

Do D.D., Weiland R.H., 1981c. Deactivation of single catalyst particles at large Thiele modulus. Travelling wave solutions. *Ind. Eng. Chem. Fundam.*, 20, 48–54. DOI: 10.1021/i100001a009.

Do D.D., 1984. Enzyme deactivation studies in a continuous stirred basket reactor. *Chem. Eng. J.*, 28(3), B51–B60. DOI: 10.1016/0300-9467(84)85063-7.

Do D.D., Weiland R.H., 1980. Consistency between rate expressions for enzyme reactions and deactivation. *Biotechnol. Bioeng.*, 22, 1087–1093. DOI: 10.1002/bit.260220515.

Do D.D., Hossain M.M., 1987. A new method to determine active enzyme distribution, effective diffusivity, rate constant for main reaction and rate constant for deactivation. *Biotechnol. Bioeng.*, 29, 545–551. DOI: 10.1002/bit.260290502.

Doran P.M., 1995. *Bioprocess engineering principles*. 1st ed., Elsevier Science & Technology Books.

Eissen M., Zogg A., Hungerbühler K., 2003. The runaway scenario in the assessment of thermal safety: Simple experimental access by means of the catalytic decomposition of H_2O_2. *J. Loss Prev. Process Ind.*, 16, 289–296. DOI: 10.1016/S0950-4230(03)00022-6.

Ene M.D., Maria G., 2012. Temperature decrease (30 – −25°C) influence on bi-enzymatic kinetics of d-glucose oxidation. *J. Mol. Catal. B: Enzym.*, 81(Supplement C), 19–24. DOI: 10.1016/j.molcatb.2012.05.001.

Farkye N.Y., 2004. Cheese technology. *Int. J. Dairy Technol.*, 57, 91–98. DOI: 10.1111/j.1471-0307.2004.00146.x.

Görenek G., Akyilmaz E., Dinckaya E., 2004. Immobilization of catalase by entrapping in alginate beads and catalase biosensor preparation for the determination of hydrogen peroxide decomposition. *Artif. Cells, Blood Substitues, Immobilization*, 32, 453–461. DOI: 10.1081/BIO-200027518.

Grigoras A. G., 2017. Catalase immobilization – A review. *Biochem. Eng. J.*, 117, Part B, 1–20. DOI: 10.1016/j.bej.2016.10.021.

Grubecki I., 2016. How to run biotransformations – At the optimal temperature control or isothermally? Mathematical assessment. *J. Process Control*, 44, 79–91. DOI: 10.1016/j.jprocont.2016.05.005.

Grubecki I., 2012. Analytical determination of the optimal temperature profiles for the reaction with parallel deactivation of enzyme encapsulated inside microorganisms cells. *Chem. Biochem. Eng. Q.*, 26(1), 31–43.

Grubecki I., 2017. External mass transfer model for hydrogen peroxide decomposition by Terminox Ultra catalase in a packed-bed reactor. *Chem. Process Eng.*, 38, 307–319. DOI: 10.1515/cpe-2017-0024.

Hassan M.M., Atiqullah M., Beg S.A., Chowdhury M.H.M., 1995. Analysis of non-isothermal tubular reactor packed with immobilized enzyme systems. *Chem. Eng. J. Biochem. Eng. J.*, 58, 275–283. DOI: 10.1016/0923-0467(95)06097-9.

Horst F., Rueda E.H., Ferreira M.L., 2006. Activity of magnetite-immobilized catalase in hydrogen peroxide decomposition. *Enzyme Microb. Technol.*, 38, 1005–1012. DOI: 10.1016/j.enzmictec.2005.08.035.

Hossain M.M., Do D.D., 1989. General theory of determining intraparticle active immobilized enzyme distribution and rate parameters. *Biotechnol. Bioeng.*, 33, 963–975. DOI: 10.1002/bit.260330805.

Illanes A., Wilson L., Vera C. (Eds.), 2013. Enzyme kinetics in a heterogeneous system, In: *Problem solving in enzyme biocatalysis*. John Wiley and Sons Ltd, 87–140.

Illanes A. (Eds.), 2013. Enzyme reactor design and operation under mass-transfer limitations, In: *Problem Solving in enzyme biocatalysis*. John Wiley and Sons Ltd, 181–202.

Karger J., Ruthven D.M., 1992. *Diffusion in zeolites and other macroporous solids*. John Wiley & Sons, Inc., USA, New York,

Krishna A.S., Kittrell J.R., 1990. Reactor analysis with diffusion-limited, concentration-dependent deactivation. *AIChE J.*, 36, 779–783. DOI: 10.1002/aic.690360516.

Lin S. H., 1991. Optimal feed temperature for an immobilized enzyme packed-bed reactor. *J. Chem. Technol. Biotechnol.*, 50, 17–26. DOI: 10.1002/jctb.280500104.

Maria G., Crisan M., 2017. Operation of a mechanically agitated semi-continuous multi-enzymatic reactor by using the Pareto-optimal multiple front method. *J. Proc. Control*, 53(Supplement C), 95–105. DOI: 10.1016/j.jprocont.2017.02.004.

Maria G., Crisan M., 2015. Evaluation of optimal operation alternatives of reactors used for d-glucose oxidation in a bi-enzymatic system with a complex deactivation kinetics. *Asia-Pac. J. Chem. Eng.*, 10(1), 22–44. DOI: 10.1002/apj.1825.

Maria G., Ene M.D., Jipa I., 2012. Modelling enzymatic oxidation of d-glucose with pyranose 2-oxidase in the presence of catalase. *J. Mol. Catal. B: Enzym.*, 74, 209–218. DOI: 10.1016/j.molcatb.2011.10.007.

Maria G., 2012. Enzymatic reactor selection and derivation of the optimal operation policy, by using a model-based modular simulation platform. *Comput. Chem. Eng.*, 36, 325–341. DOI: 10.1016/j.compchemeng.2011.06.006.

Martin A.D., 2000. Interpretation of residence time distribution data. *Chem. Eng. Sci.*, 55, 5907–5917. DOI: 10.1016/S0009-2509(00)00108-1.

O'Brien K.B., Killoran S.J., O'Neill R.D., Lowry J.P., 2007. Development and characterization in vitro of a catalase-based biosensor for hydrogen peroxide monitoring. *Biosens. Bioelectron.*, 22, 2994–3000. DOI: 10.1016/j.bios.2006.12.020.

Oh S.H., Yu H.J., Kim M.S., So S., Suh H.J., 2002. Biodegradation of hydrogen peroxide in semiconductor industrial wastewater with catalase from *Micrococcus sp*. *J. Food Sci. Nutr.*, 7, 33–36. DOI: 10.3746/jfn.2002.7.1.033.

Palazzi E., Converti A., 2001. Evaluation of diffusional resistances in the process of glucose isomerization to fructose by immobilized glucose isomerase. *Enzyme Microb. Technol.*, 28, 246–252. DOI: 10.1016/S0141-0229(00)00323-9.

Polakovic M., Vrabel P., 1996. Analysis of the mechanism and kinetics of thermal inactivation of enzymes: Critical assessment of isothermal inactivation experiments. *Process Biochem.*, 31, 787–800. DOI: 10.1016/S0032-9592(96)00026-X.

Sendín J.-O.H., Otero-Muras I., Alonso A.A., Banga J.R., 2006. Improved optimization methods for the multiobjective design of bioprocesses. *Ind. Eng. Chem. Res.*, 45, 8594–8603. DOI: 10.1021/ie0605433.

Shen L., Chen Z., 2007. Critical review of the impact of tortuosity on diffusion. *Chem. Eng. Sci.*, 62, 3748-3755. DOI: 10.1016/j.ces.2007.03.041.

Sherwood T.G., Pigford R.L., Wilke C.R., 1975. *Mass transfer*, in: Clark B.J., Maisel J.W. (Eds.). McGraw-Hill Inc., New York, USA

Soares J.C., Moreira P.R., Queiroga A.C., Morgado J., Malcata F.X., Pintado M.E., 2011. Application of immobilized enzyme technologies for the textile industry: a review. *Biocatal. Biotransform.*, 29, 223–237. DOI: 10.3109/10242422.2011.635301.

Tai N.M., Greenfield P.F., 1981. Determination of the inherent deactivation characteristics for the parallel poisoning of immobilized catalase. *Biotechnol. Bioeng.*, 23, 805–822. DOI: 10.1002/bit.260230411.

Tarhan L., Uslan A.H., 1990. Characterization and operational stability of immobilized catalase. *Process Biochem.*, 25(1), 14–18.

Testu A., Didierjean S., Maillet D., Moyne C., Metzger T., Niass T., 2007. Thermal dispersion for water or air flow through a bed of glass beads. *Int. J. Heat Mass Transfer*, 50(7–8), 1469–1484. DOI: 10.1016/j.ijheatmasstransfer.2006.09.002.

Trusek-Hołownia A., Noworyta A., 2015. Efficient utilisation of hydrogel preparations with encapsulated enzymes – A case study on catalase and hydrogen peroxide degradation. *Biotechnol. Rep.*, 6, 13–19. DOI: 10.1016/j.btre.2014.12.012.

Vasudevan P.T., Weiland R.H., 1990. Deactivation of catalase by hydrogen peroxide. *Biotechnol. Bioeng.*, 36, 783–789. DOI: 10.1002/bit.260360805.

Received 29 May 2017
Received in revised form 24 November 2017
Accepted 12 January 2018

APPENDIX A

A column (0.36 m $\times$ 8×10^{-3} m) with jacket of water recirculation, packed with non−porous glass beads (average particle diameter of 5.0×10^{-4} m) at 293 K was used to measure the longitudinal spreading of the tracer concentration (C_A) in the exit stream as a function of time (t) and then to estimate the Peclet number for mass transfer (Pe_{mL}). More details concerning the model reactor can be found in Table 2. Hydrogen peroxide solution (0.078 kmol m^{-3}) was used as a tracer. After steady liquid was attained, 1 cm^3 of the tracer was quickly injected. Injection time was kept as low as possible, to achieve almost ideal pulse input conditions. The response (H_2O_2 concentration vs. time) for the reactor outlet was monitored by means of UV–Vis Jasco V-530 spectrophotometer (Artisan T.G., Champaign IL, USA) equipped with a quartz cuvette Q11020 (Gallab, Warsaw, Poland) with optical light path of 20 mm, until the tracer concentration was reduced to near zero. The measurements were carried out at 240 nm wavelength (molar extinction coefficient of $\varepsilon_{240} = 39.4$ m^3 kmol^{-1}cm^{-1}). As a result the residence rime distribution (RTD) function $E(t)$ of the H_2O_2 solution has been determined from

$$E(t) = \frac{C_A(t)}{\int_0^\infty C_A(t)\,dt} = \frac{C_{A,i}}{\sum_i C_{A,i}\Delta t_i} \tag{A.1}$$

for all values of the volumetric flux (Q) applied. On the basis of RTD response the values of the mean residence time t_m

$$t_m = \int_0^\infty tE(t)\,dt = \frac{\sum_i t_i C_{A,i}\Delta t_i}{\sum_i C_{A,i}\Delta t_i} \tag{A.2}$$

and variance of the data σ_t^2

$$\sigma_t^2 = \int_0^\infty (t-t_m)^2 E(t)\,dt = \frac{\sum_i t_i^2 C_{A,i}\Delta t_i}{\sum_i C_{A,i}\Delta t_i} - t_m^2 \tag{A.3}$$

were assessed.

Then, using Eq. (A.4) obtained for a closed–closed system, the Peclet number (Pe_{mL}) was calculated from (Martin, 2000)

$$\sigma_\theta^2 = \frac{\sigma_t^2}{t_m^2} = \frac{2}{Pe_{mL}}\left[1 - \frac{1-\exp(-Pe_{mL})}{Pe_{mL}}\right] \tag{A.4}$$

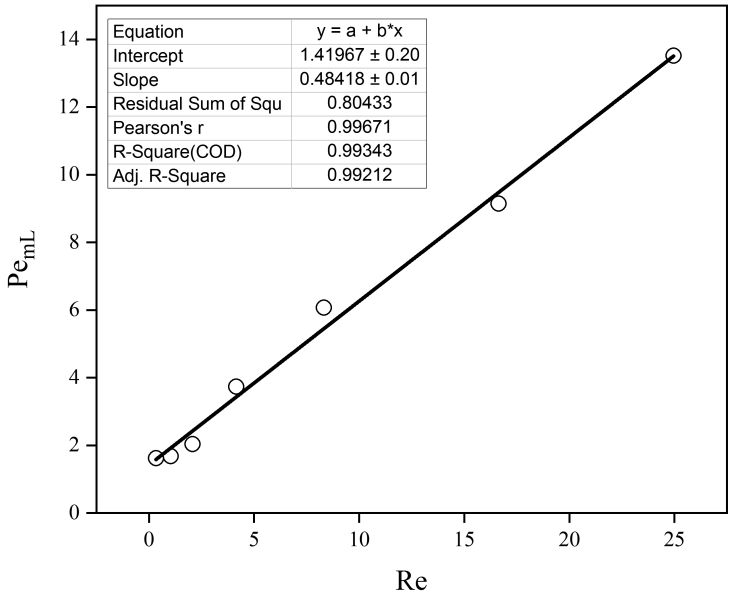

Fig. A.1. Dependence Pe_{mL} vs. Re for the model FXBR

In consequence, the dependence Pe_{mL} vs. Re with a statistical report has been depicted in Fig. A.1. Experiments were carried out at the feed flow rate ranging from 3.33×10^{-8} m^3s^{-1} to 250×10^{-8} m^3s^{-1} and controlled by a flowmeter.